Available online at www.sciencedirect.com
ScienceDirect
Tetrahedron
Tetrahedron 63 (2007) 7449–7456

Stabilization of an asymmetric bolaamphiphilic sugar-based crown ether hydrogel by hydrogen bonding interaction and its sol–gel transcription

Jong Hwa Jung,[a,*] Jeong Ah Rim,[b] Eun Jin Cho,[c] Soo Jin Lee,[a] Il Yun Jeong,[d] Naohiro Kameda,[e] Mitsutoshi Masuda[e] and Toshimi Shimizu[e]

[a]*Department of Chemistry and Research Institute of Natural Science, Gyeongsang National University, 900 Gazwa-dong, Chinju 660-701, South Korea*
[b]*Nanomaterial Team, Korea Basic Science Institute (KBSI), Daejeon 305-330, South Korea*
[c]*Department of Materials Science and Engineering, KAIST, Daejeon 305-701, South Korea*
[d]*Advanced Radiation Technology Institute, Korea Atomic Energy Research Institute, Jeongeup 580-185, South Korea*
[e]*Nanoarchitectonics Research Center (NARC), National Institute of Advanced Industrial Science and Technology (AIST), Tsukuba Central 5, 1-1-1 Higashi, Tsukuba, Ibaraki 305-8562, Japan*

Received 30 October 2006; revised 6 February 2007; accepted 9 February 2007
Available online 20 February 2007

Abstract—Asymmetric bolaamphiphilic sugar-based hydrogelators (**1**–**3**) were synthesized and their gelation ability with and without alkylammonium ions was investigated by CD, TEM, FTIR and NMR. These compounds acted as versatile gelators for organic solvents and water. The xerogels **1**–**3** obtained from water showed well-developed structures of fibrils with diameters of 10–38 nm and length of several hundred micrometers. Particularly, the gelation ability of crown-appended gelator **1** was drastically enhanced by addition of alkylammonium ions **4** and **5**, suggesting that the bridging effect of alkyldiammonium ions could be the primary driving-force for the stabilization due to the intermolecular hydrogen bonding and electrostatic interactions. The present result is a rare case of a hydrogel being stabilized by a host–guest interaction. In addition, the hydrogel **1** with $AgNO_3$ and $KClO_4$ induced the formation of nanotubular and vesicular structures of silica by sol–gel polymerization of TEOS, respectively. These results indicate that hydrogel **1** acted as a template to produce inorganic nanomaterials.

1. Introduction

Gels belong to the class of 'soft' materials that neither flow freely like a true liquid nor take on the definite shape of a rigid solid. Owing mainly to this property, gels are among the most useful supramolecular systems with wide applications in photography, drug delivery, cosmetics, sensors, and food processing, to name a few.[1] Nature itself has utilized the gel, with protoplasm being a primary example. Although gels are best known to arise from polymers, proteins, and inorganic substances, low molecular-weight organic compounds can also exhibit gelating behavior.[2–4] The organic gelators self-assemble into long fibrous structures that eventually entangle into three-dimensional networks.[5–12] Solvents contained within the interstices of the network suffer impaired flow. Thus, a ten-fold increase in viscosity, induced by only a single gelator molecule per 10^5 solvent molecules, is not uncommon.[5]

Since the stability of the product gels is closely related to the superstructures that are formed, we considered that the use of additives, which can interact with the gelators in a host–guest interaction may modify the superstructures and sensitively affect their stability. If the additives can enhance the sol–gel phase-transition temperature (T_{gel}), the fragility of the gel, a common drawback of these compounds, may be rectified to some extent. Recently, the validity of this idea was demonstrated in a few limited systems.[9] Cholesterol-based gelators having an aza-crown moiety were efficiently gelated in organic solvents mainly by the van der Waals forces between cholesterol groups. We also reported an intermolecular H-bonding between crown-appended cholesterol gelators and diamine.[13]

We have focused our research effort toward exploitation of sugar-based self-assemblies formed in water.[14] An advantage of this system is that one can systematically design various aggregates utilizing the abundant basic skeletons in the

Keywords: Bolaamphiphiles; Host–guest chemistry; Hydrogel; Self-assembly; Sol–gel transcription.
* Corresponding author. Tel.: +82 55 751 6027; fax: +82 55 758 6027; e-mail: jonghwa@gnu.ac.kr

0040–4020/$ - see front matter © 2007 Elsevier Ltd. All rights reserved.
doi:10.1016/j.tet.2007.02.068

carbohydrate family. In the process, we found that glucoside or glucosamide derivatives can gelate water in the presence of a small amount of polar organic solvent or several organic solvents.[14a,b] The findings imply that if we carefully search for sugars as well as for appropriate hydrophilic groups, several amphiphilic gelators may be discovered; this may be useful to define the basic structural requirements to design excellent amphiphilic gelators. With these objectives in mind, we designed new gelators **1**–**3** bearing an aldopyranose moiety, an aminophenyl group, and a long alkyl chain group. Also, we introduced a hydrophilic moiety such as crown ether, diamine or carboxylic acid moieties to improve the solubility in water at the end group. Particularly, the stability of the self-assembled superstructure for gelator **1** should increase by the intermolecular hydrogen bonding interaction between the crown moiety and the ammonium ion.

2. Results and discussion

2.1. Syntheses of hydrogelators

Gelators **1**–**3** were synthesized via a convergent strategy (Scheme 1) in which dodecanedioyl dichloride was attached to aminophenyl glucopyranoside using TEA mediated coupling conditions. Gelators **1** and **2** were synthesized by coupling aminobenzo-18-crown-6 and diaminoethane to **3** in excellent (50 and 90%) yield, respectively. The products were purified using silica gel column chromatography.

2.2. Gelation abilities of gelators 1–3

The gelation abilities of **1**–**3** without additives were examined in 13 different solvent systems and the results are summarized in Table 1. Commonly, **1**–**3** showed seven 'G' (stable gel) marks and four 'S' (soluble) marks. Compounds **1**–**3** can gelate water, indicating that they act as versatile gelators of various organic solvents and water. With the additives, the gel stabilities were improved, especially in water. Interestingly, the specific effect of the alkyldiammonium ions **4** and **5** appeared in DMF. The 'S' for **1** in DMF became 'PG' in the presence of **4** and **5**. This phase change is attributed to the intermolecular hydrogen bonding interaction between one ammonium and two benzo-crown ether rings. This bridging effect should result in the stabilization of the organogel state.

To explore the interaction of gelator with guest in the gel state, sol–gel phase-transition studies were carried out. The T_{gel} values were measured as a function of mole ratio of guest to gelator. The curves for **1**+**4** and **1**+**5** indicate the formations of 1:2 (guest/gelator) complexes through intermolecular hydrogen bonding interactions (Fig. 1). Accordingly, the T_{gel} values beyond mole ratio=0.5 are nearly constant, suggesting that the complexes with this stoichiometry are quite stable. The maximum values of ΔT_{gel} for **1** by addition of **4** and **5** were approximately 13 °C and 12 °C, respectively. The results suggest that the binding ability of **1** (benzo-18-crown-6) complex with **4** is similar to that of **1** complex with **5**. Also, the observation supports the idea that the bridging effects of **4** and **5** could be an additional driving-force for stabilization of the hydrogel. Addition of **6**, however, led to no significant change in the T_{gel} value of **1** (Fig. 1). The result indicates that 1:1 complex formation of **1** with **6** did not influence the gel stability.

The interactions of **1** with guests in the sol state were explored by ^{1}H NMR titrations because broadening of the corresponding resonance lines in the gel state had been observed (Supplementary data: Fig. S1). The diammonium

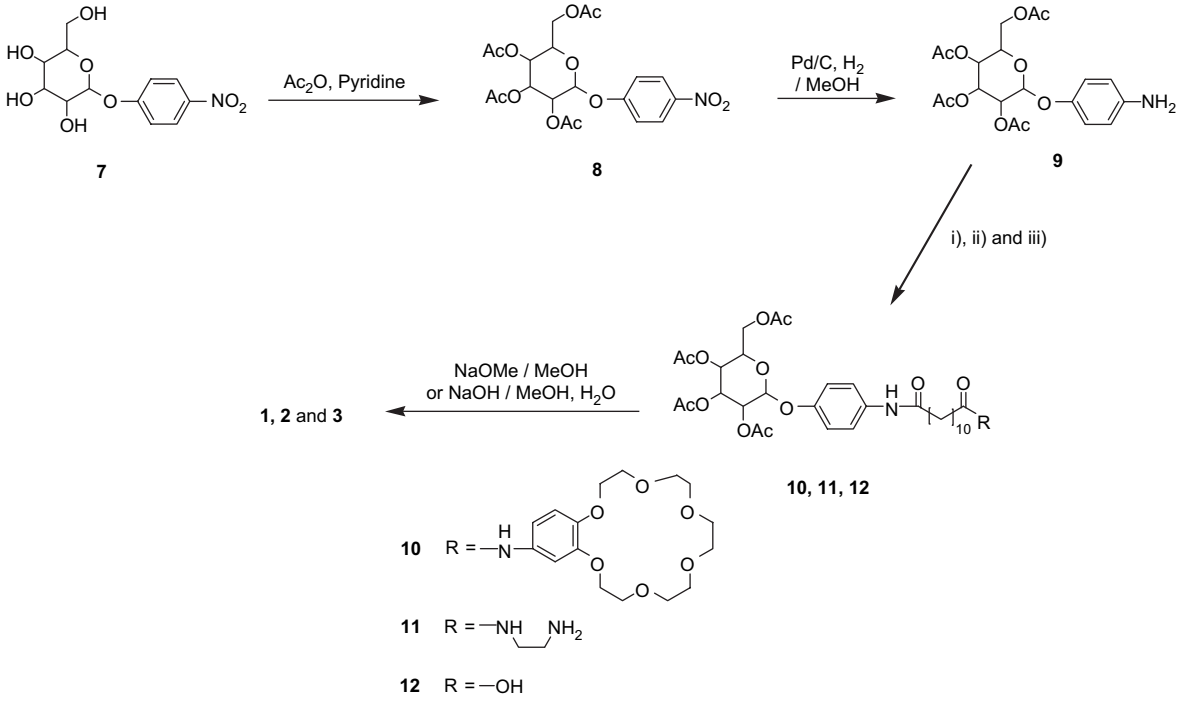

Scheme 1. Synthetic routes for **1**–**3**. Reagents and conditions: (i) dodecanedioyl dichloride, aminobenzo-18-crown-6, TEA/THF; (ii) dodecanedioyl dichloride, *N*-Boc-1,2-diaminoethane, TEA/THF, CF_3COOH/CH_2Cl_2, (iii) dodecanedioyl dichloride, TEA/THF.

Table 1. Gelation abilities of **1**–**3** in the presence of additives (**4**–**6**) at 25 °C[a]

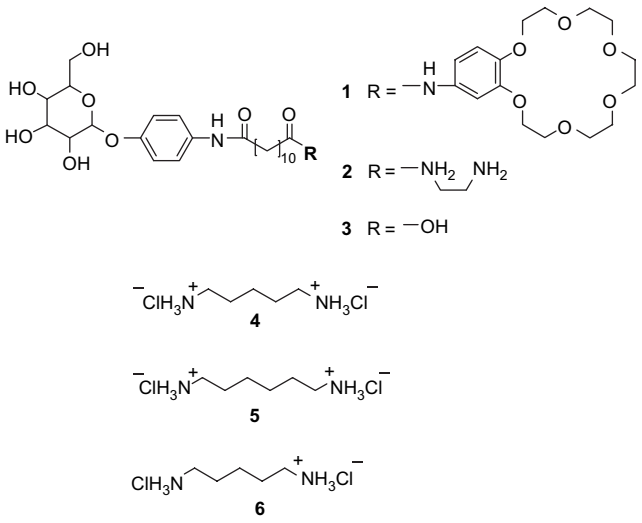

	1	1+4	1+5	1+6	2	3
Methanol	S	S	S	S	S	S
1-Butanol	G	G	G	G	G	G
1-Hexanol	G	G	G	G	G	G
THF	S	S	S	S	S	S
DMF	S	PG	PG	S	S	S
n-Hexane	I	I	I	I	I	I
Cyclohexane	I	I	I	I	I	I
Benzene	G	G	G	G	PG	G
Toluene	G	G	G	S	G	G
p-Xylene	G	G	G	G	PG	G
m-Xylene	G	G	G	G	G	G
Acetic acid	S	S	S	S	S	S
Water	G	G	G	G	G	G

[a] [Gelator]=5.0 wt %, G: stable gel; PG: partially gel, I: insoluble, S: soluble.

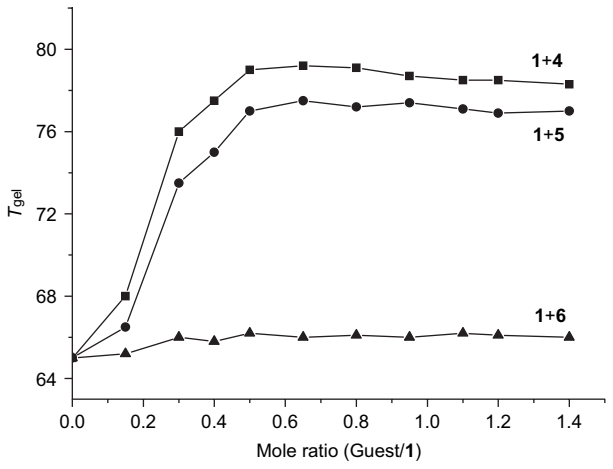

Figure 1. The T_{gel} of hydrogel **1** in the presence of **4** (1.0 wt %), **5** (1.0 wt %), and **6** (1.0 wt %).

ion of guest **4** forms a 2:1 (host/guest) complex with host **1** by intermolecular hydrogen bonding interaction. This result coincides with the stoichiometry obtained from the phase transition temperature (T_{gel}) induced by addition of **4**. Also, the CH_2 protons of the crown ether moiety of **1** were shifted to low field by addition of **4**, indicating that ammonium cation protons of **4** was bound to the oxygen atom of crown ether moiety of **1** by intermolecular hydrogen bonding interactions (Fig. S2).

According to FTIR experiment, the amide carbonyl band of the gels **1** and **2** formed in water appeared at 1648 cm^{-1} due to the strong intermolecular hydrogen bonding interaction between the amide carbonyl groups (Fig. S3), which is almost identical to the spectrum measured in the solid state (1647 cm^{-1}). The same band for the gelators **1** and **2** dissolved in methanol, however, appeared at 1657 cm^{-1} due to the weak H-bonding networks in solution.

2.3. CD studies of hydrogels 1–3

As alternative evidence for the gel stabilization of **1**–**3** by addition of **4**–**6** in the microscopic structural view, we carefully observed the CD spectra of hydrogels **1**–**3** with or without **4**–**6** as shown in Figure 2. In the CD spectrum, the $\lambda_{\theta=0}$ value appears at around 237 nm (Fig. 2A), which is consistent with the absorption maximum at λ_{max}=237 nm (Fig. 2B). All CD signals for the first Cotton effect gave a negative sign, indicating that the gelators are oriented in the anti-clockwise direction. Among hydrogels **1**–**3**, the CD intensity of the hydrogel **1** without **4**–**6** was higher than those of hydrogels **2** and **3**. The results support the idea that the hydrogel **1** forms

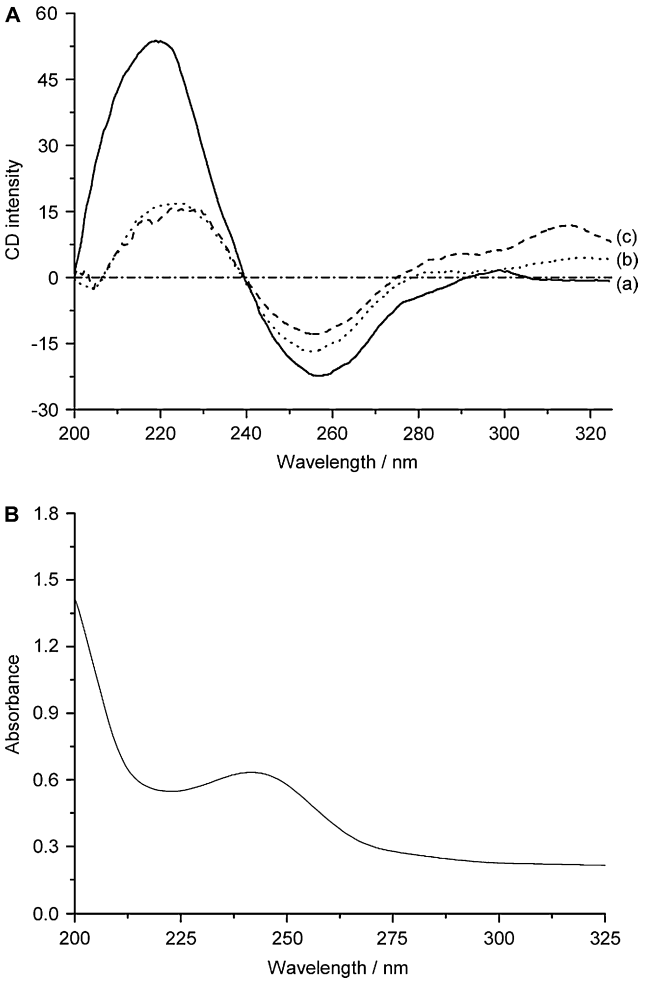

Figure 2. (A) CD spectra of hydrogels (a) **1** (1.0 wt %), (b) **2** (1.0 wt %), and (c) **3** (1.0 wt %). (B) UV–vis spectrum of hydrogel **1** (1.0 wt %).

well-ordered chiral packing structures by π–π stacking, intermolecular hydrogen bonding and hydrophobic interactions in comparison to **2** and **3**. They showed only a weak CD signal at temperatures above a phase transition temperature. The CD signal, however, became strong again when the gels formed fiber structures after several hours. However, the CD spectrum of **1** in methanol solution showed a much weaker signal, suggesting that **1** did not form well-ordered chiral packing structures.

Interestingly, the intensities for the CD spectra of the hydrogel **1** were dramatically enhanced upon addition of **4** and **5** (Fig. 3), indicating that additives **4** and **5** induce well-ordered chiral packing structure of the hydrogel **1** by 1:2 (guest/host) complex formations through intermolecular hydrogen bonding interaction. These results coincide with the stabilization obtained from the phase transition temperature (T_{gel}) induced by addition of **4** or **5**. In contrast, the intensity of the CD spectrum of the hydrogel **1** was essentially unchanged with **6**, implying that the chiral molecular packing structure of hydrogel **1** was not influenced with **6**.

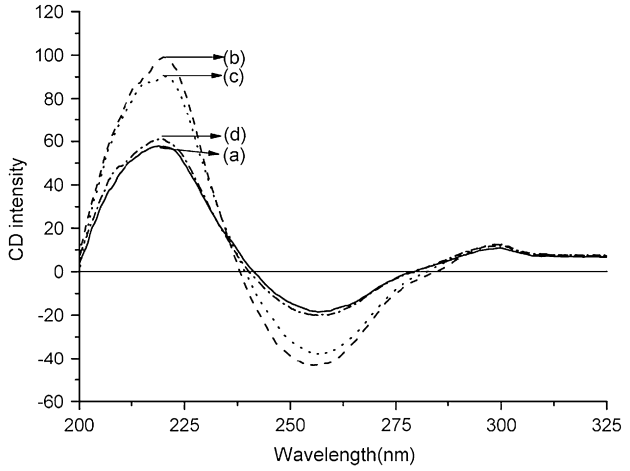

Figure 3. CD spectra of (a) hydrogels **1** (1.0 wt %), (b) **1**+**4** (2:1 equiv), (c) **1**+**5** (2:1 equiv), and (d) **1**+**6** (2:1 equiv).

2.4. Morphologies of hydrogels 1–3

The TEM images of the xerogels prepared from the frozen samples of the hydrogels were obtained (Fig. 4).[15] The xerogel **1** without guest shows a right-handed helical fiber structure with ca. 38 nm width and several hundred micrometers in length. The helicity of the fiber coincides with the helical direction obtained from CD measurement, implying that the microscopic helicity of the hydrogel **1** is reflected in the macroscopic helicity. After addition of guest **4** or **5**, however, no significant differences were found in the visual morphology of **1**. Hence, the influence induced by **4** or **5** is not so large as to change the superstructure. On the other hand, the hydrogels **2** and **3** reveal a much looser helical structure of fibrils with 10–20 nm width and several hundred micrometers in length.

Additionally, from the X-ray diffraction pattern we obtained mechanistic information[12] on the molecular packing of the gelators in the neat gel. The xerogel **1** with and without **4** obtained from water by the freezing method resulted in the sponge-like aggregate, but not the typical crystal. The small-angle diffraction patterns of **1** without **4** showed at a long period of 3.20 nm (Fig. S4), which is similar to extended length of one molecule **1** (3.41 nm the CPK molecular modeling). On the other hand, the **1**+**4** complex was only slightly smaller than that of the hydrogel **1** itself, indicating that the molecular packing structure of the hydrogel **1** was not influenced much by the addition of **4**. Hydrogelator **1** can form a complex by two different methods as shown in

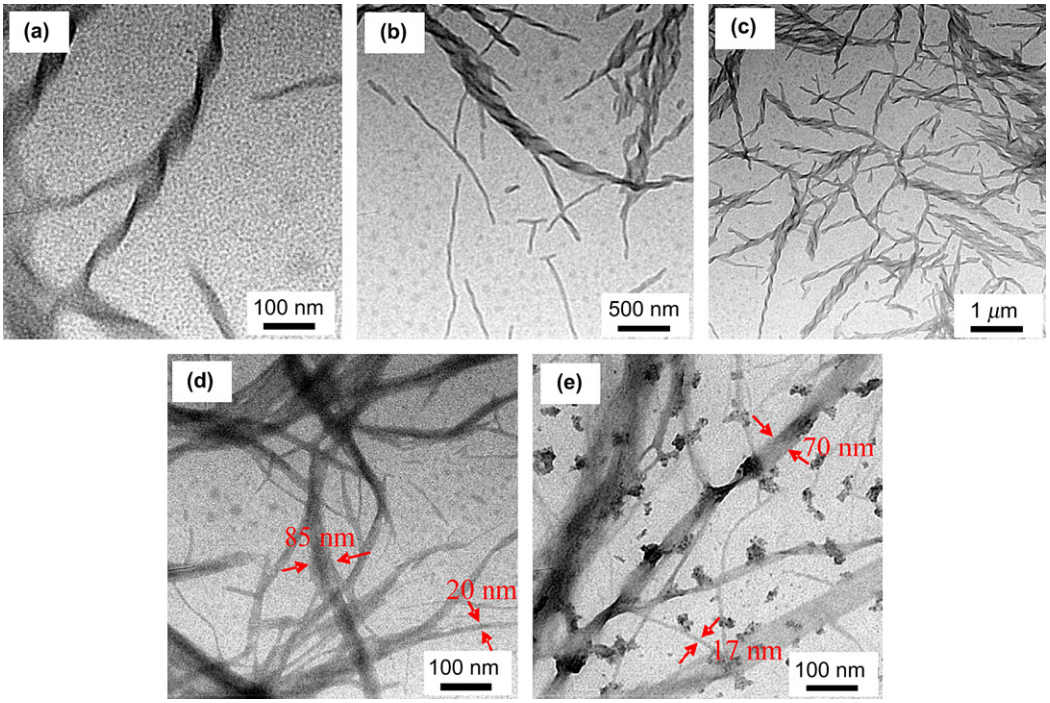

Figure 4. SEM images of (a) hydrogels **1** (1.0 wt %), (b) **1**+**4** (2:1 equiv), (c) **1**+**5** (2:1 equiv), (d) **2** (1.0 wt %), and (e) **3** (1.0 wt %).

Figure S5. One process induces a monolayered structure with head-to-head or tail-to-tail packing, the *d* distanced, which should increase, while the other induced a bilayered structure with head-to-tail packing, the *d* distanced, which is almost the same as hydrogel **1** itself. These results strongly suggest that the **1**+**4** complex forms a monolayered structure by the intermolecular hydrogen bonding interaction.

2.5. Sol–gel polymerization of TEOS using the hydrogel 1

To transcribe the novel superstructure constructed in the hydrogel to a silica nanotube, sol–gel polymerization of TEOS (tetraethyl orthosilicate) was carried out, using **1** according to a similar method to that described previously.[14] The details of the sol–gel experiments are described in Section 4.

We observed the SEM pictures of the silica obtained from hydrogel **1** in the presence of $AgNO_3$ and $KClO_4$ after calcination (Fig. 5). The silica nanotube in the presence of $AgNO_3$ showed a fibrous structure with 25–30 nm outer diameter and a few micrometers in length (Fig. 5a). The yield for the silica nanotube was ca. 95%. This result indicates that hydrogel **1** was successfully transcribed into the silica nanotube by electrostatic interaction. Furthermore, the well-defined silica before calcination showed a fibrous structure with the same size as that obtained after calcination. In contrast, a spherical structure of the silica with 150–250 nm diameter was obtained by hydrogel **1** obtained with $KClO_4$ (Fig. 5b). In order to obtain visual insights into the aggregation mode, we observed the xerogel structure of hydrogel **1** in the presence of $KClO_4$ by SEM. As expected, the xerogel **1** in the presence of $KClO_4$ showed a spherical structure with 70–80 nm outer diameter (Fig. S6). The finding indicates that hydrogel **1** with $KClO_4$ was transcribed into the silica structure by the electrostatic interaction.

To further corroborate that the hydrogel superstructure really acts as a template for the growth of the silica nanotube, we took the TEM micrograph after removal of **1** by calcination. Figure 6 shows TEM pictures of the silica obtained from hydrogel **1** in the presence of $AgNO_3$ or $KClO_4$. It is clear that the central part of the material is light and both edges are dark, implying the well-defined hollow nanotube structure. The silica nanotube possesses an inner diameter of ca. 8.5 nm (Fig. 6a). In contrast, the hollow spherical structure of the silica with 85 nm inner diameter was obtained from the hydrogel **1** with $KClO_4$ (Fig. 6b), indicating that the spherical structure of hydrogel **1** with $KClO_4$ (Fig. S6) was transcribed into the silica structure by sol–gel reaction.

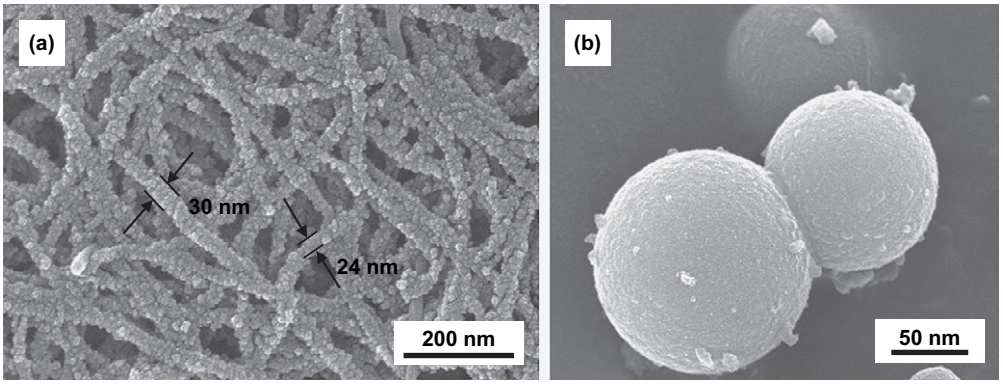

Figure 5. SEM images of the silica structures obtained from hydrogels **1**+$AgNO_3$ and (b) **1**+$KClO_4$ by sol–gel transcription.

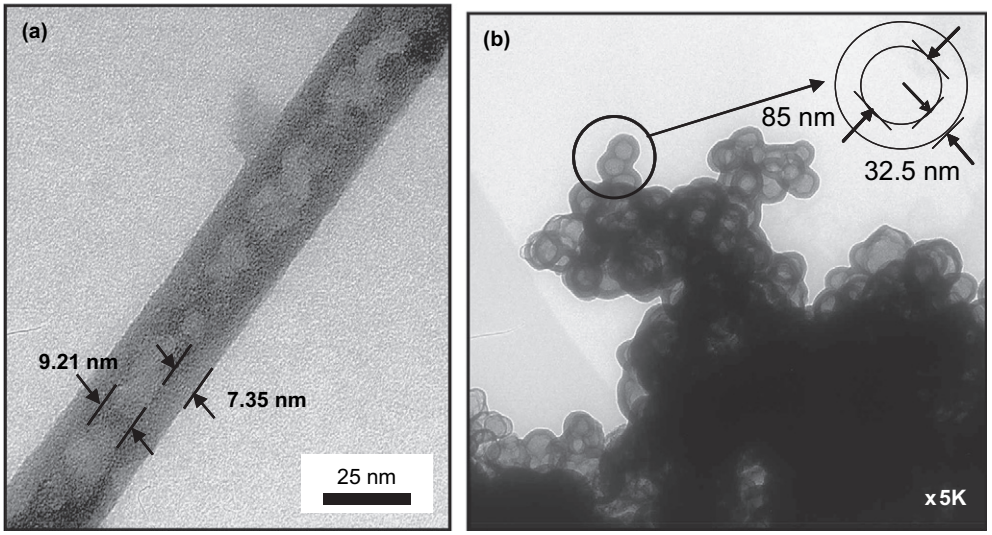

Figure 6. TEM images of the silica structures obtained from hydrogels **1**+$AgNO_3$ and (b) **1**+$KClO_4$ by sol–gel transcription after calcination.

3. Conclusions

We have demonstrated the remarkable stabilization of the sugar-based crown ether hydrogel **1** in the presence of alkyldiammonium ions **4** and **5** as guests. On the basis of the sol–gel phase transition, NMR and XRD results, the host–guest type interaction stabilizes the proposed hydrogel by synergic effects of H-bonds. Hydrogel **1** in the presence and in the absence of guest molecules formed a helical fiber structure. Furthermore, the sugar-based hydrogelators **1**–**3** can gelate several solvents selectively. Hydrogel **1** in the presence of $AgNO_3$ or $KClO_4$ induced either the silica nanotube or vesicles, respectively, by sol–gel polymerization of TEOS.

To the best of our knowledge, this is a rare example exhibiting gelation ability controlled by host–guest type molecular recognition. This finding suggests that the phase transition of the gels induced by the host–guest interaction could be applicable to drug delivery systems, collection of waste materials and pollutants, and recovery of precious bio-active compounds, etc.[16]

4. Experimental

4.1. Apparatus for spectroscopy measurements

^1H and ^{13}C NMR spectra were measured on a Bruker ARX 300 apparatus. IR spectra were obtained in KBr pellets using a Shimadzu FTIR 8100 spectrometer, and MS spectra were obtained by a Hitachi M-250 mass spectrometer. Circular dichroism (CD) spectra were measured on a JASCO J-820KS spectrophotometer (cell diameter 10 mm).

4.2. SEM and TEM measurements

For energy-filtering transmission electron microscopy (EF-TEM) a piece of the gel was placed on a carbon-coating copper grid (400 mesh) and removed after 1 min, leaving some small patches of the gel on the grid. This was then dried for 1 h at low pressure. The specimen was examined with Carl Zeiss EM902, using accelerating voltage of 80 kV and a 16 mm working distance. Field emission scanning electron microscope (FE-SEM) was taken on Hitachi S-4500. To observe morphology of the silica nanotube, the samples were prepared by adhering a large number of the silica particles before and after calcination onto a carbon film on a Cu grid.

4.3. Gelation test of organic fluids

The gelator and the solvent were put in a septum-capped test tube and heated in an oil bath until the solid was dissolved. The solution was cooled at room temperature. If the stable gel was observed at this stage, it was classified as G in Table 1.

4.4. Sol–gel polymerization of TEOS

Compound **1** (2–5 mg) and $AgNO_3$ or $KClO_4$ (1.5 equiv) were dissolved in water (200–500 mg) by heating. The gel sample was cooled to room temperature. TEOS (20–50 mg) and benzylamine as a catalyst were added to the gel sample. The sample was heated until a clear solution was obtained and then left at ambient temperature for 2–7 days. Subsequently, the sample was heated at 200 °C for 2 h and 500 °C for 2 h under a nitrogen atmosphere and then kept at 500 °C under aerobic conditions for 4 h.

5. Synthesis

Compounds **4**–**7** are commercially available.

5.1. Compound 1

A mixture of **10** (0.80 g, 0.83 mmol) and NaOMe in MeOH (0.5 M, 4 mL) was stirred for 1 h at room temperature. The solution was concentrated in vacuo, and acidified with 0.1 M HCl solution. The precipitate was filtered and purified by column chromatography (CH_2Cl_2/MeOH, 10:1 v/v) to yield **1** (0.25 g, 50%) as light yellow solid. Mp: 190–191 °C. ^1H NMR (300 MHz, DMSO-d_6): δ 9.79 (s, 1H, –NH), 9.75 (s, 1H, –NH), 7.48 (d, 2H, J=9.0, ArH), 7.31 (s, 1H, ArH), 7.07 (d, 1H, J=8.4, ArH), 6.95 (d, 1H, J=9.0, ArH), 6.86 (d, 2H, J=9.0, ArH), 5.30 (d, 1H, J=5.1, –OH), 5.04 (d, 1H, J=5.1, –OH), 4.76 (d, 1H, J=7.2, –OH), 4.58 (t, 1H, J=7.2, –OH), 4.12 (q, 1H, J=5.4, –CH–), 4.03–3.98 (m, 6H, –CH– and –CH_2–), 3.78–3.73 (m, 7H, –CH– and –CH_2–), 3.38–3.31 (m, 12H, –CH_2–), 2.29–2.22 (m, 4H, –CH_2–), 1.61–1.52 (m, 4H, –CH_2–), 1.27 (s, 12H, –CH_2–); IR (KBr) 3436, 2919, 2849, 2360, 2332, 1648, 1532 cm^{-1}; MS (FAB): 793 $(M+H)^+$ (calcd MW=792.91); elemental analysis calcd (%) for $C_{40}H_{60}N_2O_{14}$: C 60.59, H 7.63, N 3.53, O 28.25; found: C 60.16, H 6.99, N 3.38.

5.2. Compound 2

A mixture of **11** (0.80 g, 0.83 mmol) and NaOMe in MeOH (1 mL, 0.5 M) was stirred for 1 h at room temperature. The solution was concentrated in vacuo, and acidified with 0.1 M HCl solution. The precipitate was filtered and dried in vacuo, pale yellow solid. Yield 90%. Mp: 205–206 °C. ^1H NMR (300 MHz, DMSO-d_6): δ 9.81 (s, 1H, –NH), 9.43 (s, 1H, –NH), 7.54 (d, 2H, J=9.0, ArH), 6.93 (d, 2H, J=9.0, ArH), 5.28–5.22 (m, 1H, –OH), 5.01–4.98 (m, 1H, –OH), 4.69–4.67 (m, 1H, –OH), 4.56–4.51 (m, 1H, –OH), 4.12 (q, 1H, J=5.4, –CH–), 3.79–3.72 (m, 6H, –CH– and –CH_2–), 2.27–2.22 (m, 4H, –CH_2–), 2.17–2.14 (m, 4H, –CH_2–), 1.54–1.50 (m, 4H, –CH_2–), 1.32 (s, 12H, –CH_2–); MS (FAB): 793 $(M+H)^+$ (calcd MW=792.91); elemental analysis calcd (%) for $C_{26}H_{43}N_3O_8$: C 59.41, H 8.25, N 7.99; found: C 60.02, H 8.13, N 7.94.

5.3. Compound 3

A mixture of **12** (0.23 g, 0.35 mmol) and NaOH (0.059 g) in MeOH/H_2O (20 mL, 9:1 v/v) was stirred for 1 h at room temperature. The solution was concentrated in vacuo, and acidified with 0.1 M HCl solution. The precipitate was filtered and dried in vacuo. Mp: 124 °C. Yield 87%. ^1H NMR (300 MHz, DMSO-d_6): δ 11.95 (s, 1H, –OH), 9.72 (s, 1H, –NH), 7.47 (d, 2H, J=9, ArH), 6.95 (d, 2H, J=9, ArH), 5.26 (d, 1H, J=4.8, –OH), 5.05 (d, 1H, J=4.5, –OH), 4.98 (d, 1H, J=5.1, –OH), 4.76 (d, 1H, J=7.5, –CH–), 4.54 (t, 1H, J=5.1, –OH), 3.71–3.63 (m, 1H,

–CH–), 3.48–3.43 (m, 1H, –CH–), 3.20–3.16 (m, 4H, –CH– and $–CH_2–$), 1.50–1.43 (m, 8H, $–CH_2–$), 1.24 (s, 12H, $–CH_2–$); MS (FAB): 524 $(M+H)^+$ (calcd MW=525.25); elemental analysis calcd (%) for $C_{24}H_{37}NO_9$: C 59.61, H 7.71, N 2.90, O 29.78; found: C 59.28, H 7.17, N 2.23.

5.4. Compound 8

Nitrophenyl-β-D-glucopyranoside **7** (1.0 g, 2.54 mmol) was dissolved in pyridine (1.0 mL) and acetylacetone (1.0 mL). The reaction mixture was allowed to stand overnight and was then evaporated in vacuo to dryness with dry toluene. The residue was purified by column chromatography on silica gel with EA/Hx (1:1 v/v, R_f=0.5). Yield 75%. ^{1}H NMR (300 MHz, $CDCl_3$): δ 7.23 (d, 2H, J=9.0, Ar*H*), 7.08 (d, 2H, J=9.0, Ar*H*), 5.27–5.21 (m, 3H), 5.04 (d, 1H, J=9.0), 4.30–4.14 (m, 2H), 3.90–3.86 (m, 1H), 1.97 (s, 12H); ^{13}C NMR (75 MHz, $CDCl_3$): 170.5, 158.6, 130.5, 123.1, 115.3, 98.1, 71.4, 68.3, 65.4, 20.8, 19.6 ppm; MS (FAB): 470 $(M+H)^+$ (calcd MW=469.1); elemental analysis calcd (%) for $C_{20}H_{23}NO_{12}$: C 51.18, H 4.94, N 2.98; found: C 51.01, H 5.24, N 2.86.

5.5. Compound 9

Compound **8** (1.0 g) was dissolved in MeOH (25 mL). After 5 min of N_2 purging, Pd on activated carbon (10 wt %, 100 mg) was added. Under 2 atm of H_2, the reaction was allowed to proceed for 3 h. After filtration and evaporation, pure **9** was obtained as a pale yellow solid (2.48 g, quantitative). EA/Hx (1:1 v/v, R_f=0.5). Yield 75%. ^{1}H NMR (300 MHz, $CDCl_3$): δ 6.85 (d, 2H, J=9.0, Ar*H*), 6.64 (d, 2H, J=9.0, Ar*H*), 5.31–5.13 (m, 3H), 4.96 (d, 1H, J=9.0), 4.32–4.19 (m, 2H), 3.82–3.77 (m, 1H), 3.48 (s, 2H), 2.05 (s, 12H); ^{13}C NMR (75 MHz, $CDCl_3$): 170.3, 158.9, 130.2, 121.0, 119.3, 97.1, 73.4, 69.1, 64.6, 20.5, 19.1 ppm; MS (FAB): 438 $(M+H)^+$ (calcd MW=439.1); elemental analysis calcd (%) for $C_{20}H_{25}NO_{10}$: C 54.67, H 5.73, N 3.19; found: C 54.89, H 6.10, N 3.40.

5.6. Compound 10

Dodecanedioyl dichloride (0.62 g, 2.32 mmol) in dry THF (8 mL) was cooled to 0 °C, and a solution of **9** (1.0 g, 2.28 mmol) and Et_3N (0.23 g, 2.28 mmol) in THF (8 mL) was added dropwise over a period of 1 h and stirred for further 2 h. A solution of amino-18-crown-6 (0.74 g, 2.26 mmol) and Et_3N (0.23 g, 2.29 mmol) in THF (5 mL) was added at once. The mixture was left to reach room temperature slowly and stirred for 18 h. The precipitate formed was filtered off and the residue obtained after evaporation of the solvent purified by column chromatography (CH_2Cl_2/MeOH, 10:1 v/v, R_f=0.4) to yield **10** (0.80 g, 37%) as light yellow solid. ^{1}H NMR (300 MHz, DMSO-d_6): δ 9.84 (s, 1H, –NH), 9.73 (s, 1H, –NH), 7.53 (d, 2H, J=9, ArH), 7.33 (s, 1H, ArH), 7.08 (d, 1H, J=8.7, ArH), 6.93 (d, 1H, J=9, ArH), 6.86 (d, 2H, J=9, ArH), 5.44 (d, 1H, J=8.1, –CH–), 5.37 (d, 1H, J=9.6, –CH–), 5.05–4.96 (m, 2H, –CH), 4.21 (d, 2H, J=9, $–CH_2–$), 4.10 (d, 1H, J=5.2, –CH–), 4.06–4.01 (m, 4H, $–CH_2–$), 3.79–3.73 (m, 4H, $–CH_2–$), 3.62–3.54 (m, 12H, $–CH_2–$), 2.25 (q, 4H, $–CH_2–$), 2.03 (s, 12H, $–CH_3$), 1.61–1.52 (m, 4H, $–CH_2–$), 1.27 (s, 12H, $–CH_2–$).

5.7. Compound 11

Dodecanedioyl dichloride (0.30 g, 1.12 mmol) in dry THF (8 mL) was cooled to 0 °C, and a solution of **9** (0.5 g, 1.13 mmol) and Et_3N (0.12 g, 1.14 mmol) in THF (8 mL) was added dropwise over a period of 1 h and stirred for further 2 h. A solution of *N*-Boc-1,2-diaminoethane (0.18 g, 1.13 mmol) and Et_3N (0.12 g, 1.14 mmol) in THF (5 mL) was added at once. The mixture was left to reach room temperature slowly and stirred for 18 h. The precipitate formed was filtered off and the residue obtained after evaporation of the solvent. The reaction mixture was stirred with CF_3COOH (5 mL) and CH_2Cl_2 (5 mL) at room temperature for 5 h. The solvents were evaporated to dryness to yield a colorless syrup. Yield 50%. ^{1}H NMR (300 MHz, DMSO-d_6): δ 9.82 (s, 1H, –NH), 9.65 (s, 1H, –NH), 7.33 (d, 2H, ArH), 7.08 (d, 2H, J=8.7, ArH), 5.36 (d, 1H, J=9.6, –CH–), 5.04–4.98 (m, 2H, –CH), 4.68 (d, 1H, J=9, $–CH_2–$), 4.65 (d, 1H, J=5.2, –CH–), 4.08–4.02 (m, 2H, $–CH_2–$), 3.50–3.42 (m, 2H), 3.01–2.92 (m, 2H), 2.30–2.26 (m, 2H, $–CH_2–$), 2.22–2.16 (m, 2H), 2.06 (s, 12H, $–CH_3$), 1.56–1.52 (m, 4H, $–CH_2–$), 1.30 (s, 12H, $–CH_2–$).

5.8. Compound 12

Dodecanedioyl dichloride (1.21 g, 4.52 mmol) in dry THF (8 mL) was cooled to 0 °C, and a solution of **9** (0.5 g, 1.14 mmol) and Et_3N (0.12 g, 1.22 mmol) in THF (8 mL) was added dropwise over a period of 1 h and stirred for further 2 h. A solution of amino-18-crown-6 (0.74 g, 2.26 mmol) and Et_3N (0.23 g, 2.29 mmol) in THF (5 mL) was added at once. The mixture was left to reach room temperature slowly and stirred for 18 h. The precipitate formed was filtered off and the residue obtained after evaporation of the solvent purified by column chromatography (CH_2Cl_2/MeOH, 10:1 v/v, R_f=0.5) to yield **7** (0.80 g, 37%) as gray solid. ^{1}H NMR (300 MHz, $CDCl_3$): δ 9.48 (s, 1H, –NH), 7.38 (d, 2H, ArH), 6.98 (d, 2H, J=8.7, ArH), 5.84 (d, 1H, J=9.6, –CH–), 5.04–4.98 (m, 2H, –CH), 4.68 (d, 1H, J=9, $–CH_2–$), 4.65 (d, 1H, J=5.2, –CH–), 4.08–4.02 (m, 2H, $–CH_2–$), 2.27–2.22 (m, 2H, $–CH_2–$), 2.19–2.15 (m, 2H), 2.06 (s, 12H, $–CH_3$), 1.55–1.50 (m, 4H, $–CH_2–$), 1.28 (s, 12H, $–CH_2–$).

Acknowledgements

This work was supported by a Korea Research Foundation Grant (KRF-2004-015-C00242) and KOSEF (R01-2005-000-10229-0).

Supplementary data

Supplementary data associated with this article can be found in the online version, at doi:10.1016/j.tet.2007.02.068.

References and notes

1. van Esch, J.; Feringa, B. L. *Angew. Chem., Int. Ed.* **2000**, *39*, 2263–2266.
2. Schoonbeek, F. S.; van Esch, J.; Hulst, R.; Kellogg, R. M.; Feringa, B. L. *Chem.—Eur. J.* **2000**, *6*, 2633–2643.

3. Hanabusa, K.; Shimura, K.; Kimura, M.; Shirai, H. *Chem. Lett.* **1996**, 885–886.
4. Murdam, S.; Greoriadis, G.; Florence, A. T. *J. Pharm. Sci.* **1999**, *88*, 608–614.
5. (a) Terech, P.; Bordas, D.; Rossat, C. *Langmuir* **2000**, *16*, 4485–4494; (b) Bhosale, S.; Bhosale, S.; Wang, T.; Kopaczynska, M.; Fuhrhop, J.-H. *J. Am. Chem. Soc.* **2006**, *128*, 2156–2157.
6. (a) Murata, K.; Aoki, M.; Suzuki, T.; Harada, T.; Kawabata, H.; Komori, T.; Ohseto, F.; Ueda, K.; Shinkai, S. *J. Am. Chem. Soc.* **1994**, *116*, 6664–6676 and references therein; (b) James, T. D.; Murata, K.; Harada, T.; Ueda, K.; Shinkai, S. *Chem. Lett.* **1994**, 273–276; (c) Jeong, S. W.; Murata, K.; Shinkai, S. *Supramol. Sci.* **1996**, *3*, 83–86; (d) Yoza, K.; Amanokura, N.; Ono, Y.; Akao, T.; Shinmori, H.; Takeuchi, M.; Shinkai, S.; Reinhoudt, D. L. *Chem.—Eur. J.* **1999**, *5*, 2722–2729.
7. (a) Wang, R.; Geiger, C.; Chen, L.; Swanson, B.; Whitten, D. G. *J. Am. Chem. Soc.* **2000**, *122*, 2399–2400; (b) Duncan, D. C.; Whitten, D. G. *Langmuir* **2000**, *16*, 6445–6452; (c) Geiger, C.; Stanescu, M.; Chen, L.; Whitten, D. G. *Langmuir* **1999**, *15*, 2241–2245.
8. (a) For recent comprehensive reviews, see: Terech, P.; Weiss, R. G. *Chem. Rev.* **1997**, *97*, 3313–3362; (b) Otsuni, E.; Kamaras, P.; Weiss, R. G. *Angew. Chem., Int. Ed.* **1996**, *35*, 1324–1326 and references therein; (c) Terech, P.; Furman, I.; Weiss, R. G. *J. Phys. Chem.* **1995**, *99*, 9558–9566 and references therein; (d) Abdallach, D. J.; Weiss, D. G. *Adv. Mater.* **2000**, *12*, 1237–1247.
9. (a) Dykes, G. M.; Smith, D. K. *Tetrahedron* **2003**, *59*, 3999–4009; (b) Smith, D. K. *Chem. Commun.* **2006**, 34–44; (c) Dykes, G. M.; Smith, D. K.; Seeley, G. J. *Angew. Chem., Int. Ed.* **2002**, *41*, 3254–3257; (d) Hirst, A. R.; Smith, D. K. *Chem.—Eur. J.* **2005**, *11*, 5496–5508.
10. (a) Melendez, R.; Geib, S. J.; Hamilton, A. D. *Molecular Self-Assembly Organic Versus Inorganic Approaches*; Fujita, M., Ed.; Springer: Berlin, New York, NY, 2000; (b) Carr, A. J.; Melendez, R.; Geib, S. J.; Hamilton, A. D. *Tetrahedron Lett.* **1998**, *39*, 7447–7450; (c) Shi, C.; Kilic, S.; Xu, J.; Enick, R. M.; Beckman, E. J.; Carr, A. J.; Melendez, R. E.; Hamilton, R. A. D. *Science* **1999**, *286*, 1540–1543; (d) Hafkamp, R. J. H.; Kokke, B. P. A.; Danke, I. M.; Geurts, H. P. M.; Rowan, A. E.; Feiters, M. C.; Nolte, R. J. *Chem. Commun.* **1997**, 545–546.
11. (a) Suzuki, M.; Nakajima, Y.; Yumoto, M.; Kimura, M.; Shirai, H.; Hanabusa, K. *Langmuir* **2003**, *19*, 8622–8624; (b) Suzuki, M.; Nakajima, Y.; Yumoto, M.; Kimura, M.; Shirai, H.; Hanabusa, K. *Chem.—Eur. J.* **2003**, *9*, 348–354.
12. (a) John, G.; Masuda, M.; Okada, Y.; Yase, K.; Shimizu, T. *Adv. Mater.* **2001**, *13*, 715–718; (b) Masuda, M.; Hanada, T.; Okada, Y.; Yase, K.; Shimizu, T. *Macromolecules* **2000**, *33*, 9233–9238; (c) Nakazawa, I.; Masuda, M.; Okada, Y.; Hanada, T.; Yase, K.; Asai, M.; Shimizu, T. *Langmuir* **1999**, *15*, 4757–4764; (d) Shimizu, T.; Masuda, M. *J. Am. Chem. Soc.* **1997**, *119*, 2812–2818; (e) Jung, J. H.; John, G.; Masuda, M.; Yoshida, K.; Shinkai, S.; Shimizu, T. *Langmuir* **2001**, *17*, 7229–7232.
13. (a) Jung, J. H.; Ono, Y.; Shinkai, S. *Tetrahedron Lett.* **1999**, *40*, 8395–8399; (b) Jung, J. H.; Lee, S. J.; Rim, J. A.; Lee, H.; Bae, T.-S.; Lee, S. S.; Shinkai, S. *Chem. Mater.* **2005**, *17*, 459–462.
14. (a) Jung, J. H.; Kobayashi, H.; Masuda, M.; Shimizu, T.; Shinkai, S. *J. Am. Chem. Soc.* **2001**, *123*, 8785–8789 and references therein; (b) Jung, J. H.; Ono, Y.; Hanabusa, K.; Shinkai, S. *J. Am. Chem. Soc.* **2000**, *122*, 5008–5009.
15. Jung, J. H.; Shinkai, S. *Top. Curr. Chem.* **2004**, *248*, 223–260.
16. Xing, B.; Yu, C.-W.; Chow, K.-H.; Ho, P.-L.; Fu, D.; Xu, B. *J. Am. Chem. Soc.* **2002**, *124*, 14846–14847; (b) van Bommel, K. J. C.; van der Pol, C.; Muizebelt, I.; Friggeri, A.; Heeres, A.; Meetsma, A.; Feringa, B. L.; van Esch, J. *Angew. Chem., Int. Ed.* **2004**, *43*, 1663–1667; (c) Tiller, J. C. *Angew. Chem., Int. Ed.* **2003**, *42*, 3072–3075.